

# The Effect of Rh on the Interaction of Co with Al<sub>2</sub>O<sub>3</sub> and CeO<sub>2</sub> Supports

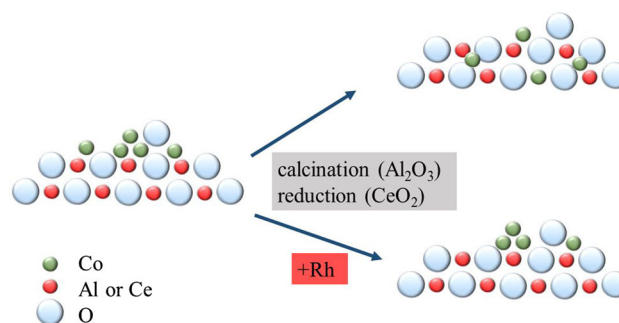
Erika Varga<sup>1</sup> · Kornélia Baán<sup>1</sup> · Gergely Ferenc Samu<sup>1,2</sup> · András Erdőhelyi<sup>1</sup> · Albert Oszkó<sup>1</sup> · Zoltán Kónya<sup>3,4</sup> · János Kiss<sup>1,4</sup>

Received: 13 April 2016 / Accepted: 7 July 2016  
© Springer Science+Business Media New York 2016

**Abstract** Co and Rh+Co catalysts supported on Al<sub>2</sub>O<sub>3</sub> and CeO<sub>2</sub> were investigated by temperature programmed reduction (TPR) and X-ray photoelectron spectroscopy (XPS). The CeO<sub>2</sub> defects, resulted from the effects of the metals, were further analyzed by Raman spectroscopy and optical absorption. Although the interaction of Co with these two supports is fairly different, it can be concluded that Rh inhibits the strong Co-support interaction. It was revealed that Co over Al<sub>2</sub>O<sub>3</sub> forms mainly Co<sup>2+</sup> compounds, only a smaller fraction of cobalt is in metallic state. After the addition of 0.1 % Rh, Co<sub>3</sub>O<sub>4</sub> like species is dominant, the amount of metallic state increased after reduction. Over CeO<sub>2</sub> the Co dissolution into the support was inhibited by Rh. A wide range of TPR results proved the stepwise reduction of Co, which was promoted by the addition of Rh. By Rh the entire mechanism of this process was altered that can be observed even by XPS. On the basis of the Raman and the optical measurements we concluded that the metals induce defect sites on the CeO<sub>2</sub> surface, and these appear as similar features on the spectra of Co and Rh containing samples, thus their density depends on the metal loading and not on the metal type. CeO<sub>2</sub> has a bandgap of 3.27 eV, which is not

altered by the metals, but an electronic contact was detected between the metals and CeO<sub>2</sub> by photovoltammetry. The increased number of metallic species is mainly responsible for the higher catalytic activity and for the enhanced hydrogen selectivity in the stream reforming of ethanol.

## Graphical Abstract



**Keywords** Rh-Co · CoAl<sub>2</sub>O<sub>4</sub> · CeO<sub>2</sub> defects · TPR · Bandgap · Photovoltammetry

## 1 Introduction

In heterogeneous catalysis the application of complex catalysts, such as supported or bimetallic systems, has resulted in significant progress in efficiency and even stability [1–4]. The role of the different oxide supports is not only to hinder the sintering of the metal particles, but also to have electronic and steric contact with them [5]. Moreover, some important reaction steps take place over the support or the metal-support interface, such as the ethylene or acetaldehyde formation from ethanol, the oxidation of CO, and the dissociation of water [6–9].

✉ János Kiss  
jkiss@chem.u-szeged.hu

<sup>1</sup> Department of Physical Chemistry and Materials Science, University of Szeged, Aradi vértanúk tere 1, Szeged 6720, Hungary  
<sup>2</sup> MTA-SZTE “Lendület” Photoelectrochemistry Research Group, Rerrich B. tér 1, Szeged 6720, Hungary  
<sup>3</sup> Department of Applied and Environmental Chemistry, University of Szeged, Rerrich B. tér 1, Szeged 6720, Hungary  
<sup>4</sup> MTA-SZTE Reaction Kinetics and Surface Chemistry Research Group, Rerrich B. tér 1, Szeged 6720, Hungary

In addition to the support effect, the physical, chemical and catalytic behavior of a metal can be gently tuned by a second metal, especially by noble metal promoters. Thus, by the addition of trace amounts of the precious component to a cheaper metal, like transition metals, catalyst with high activity at low costs could be developed. The effect of the promoter manifests in the activation of hydrogen during pretreatments causing enhanced reduction, changing the particle size distribution or they can induce electronic interaction as well as alloy formation [10, 11].

Regarding the base metal, beside the highly efficient Ni, Co has gained attention in the last few years. It should be mentioned that Co supported on  $\text{Al}_2\text{O}_3$  or  $\text{SiO}_2$  is at least as active in the Fischer–Tropsch synthesis as the classical Fe systems, although the reaction pathways are different [12]. According to some former results this reaction is enhanced with increasing the Co particle size and the ratio of the metallic cobalt, as the active form is the  $\text{Co}^0$  and the small particles tend to oxidize [13, 14]. From this point of view the addition of noble metal promoters can facilitate the reaction by enhancing the reduction. Similar considerations can be made with the dry reforming of  $\text{CH}_4$  [15, 16]. However, in ethanol involving reactions the acidic  $\text{Al}_2\text{O}_3$  favors the dehydration of the molecule and the polymerization of the resulting ethylene, causing significant carbon deposits [17, 18].

Co has been tried in the stream reforming of ethanol (SRE), too. At low Co content the product distribution was determined by the support, the main product was ethylene when supported on  $\text{Al}_2\text{O}_3$ , but acetone and a high portion of  $\text{H}_2$  were formed over Co/ $\text{CeO}_2$ . The latter effect was improved by the addition of 0.1 % Rh [19]. In the literature there is a disagreement relating to the active centers of Co: some authors suggest that  $\text{Co}^0$  is responsible for coke formation thus blocks the reaction. Others claim that metallic Co is the necessary form for the SRE [20, 21]. In some cases both  $\text{Co}^0$  and oxidized Co were present during the reaction [22, 23]. Nevertheless, it is clear that the addition of the noble metals enhances the reduction of  $\text{CoO}_x$  to metallic Co and the efficiency is improved in the SRE and oxidative SRE [24–26].

Despite the large number of studies published in this topic, the accurate nature of the relationship between Co and noble metals in bimetallic systems is still not fully understood. In the present paper we show some comparative results of  $\text{Al}_2\text{O}_3$  and  $\text{CeO}_2$  supported Co and Rh–Co catalysts, and demonstrate how the addition of Rh promoter changes the oxidation state of Co and its interaction with the support. As  $\text{CeO}_2$  is a promising candidate as a photocatalyst, we carried out some electrochemical measurements to reveal the effects of the Co and Rh on the electronic structure of this support.

## 2 Experimental

The catalysts were prepared by impregnating the supports ( $\text{Al}_2\text{O}_3$ , Degussa P110 C1,  $100 \text{ m}^2 \text{ g}^{-1}$  or  $\text{CeO}_2$ , Alfa Aesar,  $43 \text{ m}^2 \text{ g}^{-1}$ ) with the aqueous solution of  $\text{Co}(\text{NO}_3)_2$  to yield a nominal metal content of 2 or 10 wt%. The impregnated powders were dried at 383 K and calcined at 973 K. The bimetallic Rh–Co samples were prepared by sequential impregnation (impregnation with Co and calcination first, then impregnation with Rh). Before the measurements, the samples were oxidized at 673 K in flowing  $\text{O}_2$  for 20 min and reduced at 773 K in  $\text{H}_2$  for 60 min.

Temperature programmed reduction experiments were carried out by a BELCAT-A instrument, in a reactor (quartz tube 9 mm outer diameter) that was externally heated. Before the measurements, the catalysts were treated in  $\text{O}_2$  at 673 K for 30 min. Thereafter, the samples were cooled in flowing Ar to room temperature and let the temperature equilibrate for 15 min. The oxidized sample was flushed with Ar containing 10 %  $\text{H}_2$ , the reactor was heated linearly at a rate of  $20 \text{ K min}^{-1}$  up to 1373 K and the  $\text{H}_2$  consumption was detected by a thermal conductivity detector.

XP spectra were taken with a SPECS instrument equipped with a PHOIBOS 150 MCD 9 hemispherical electron energy analyzer, using Al  $\text{K}_\alpha$  radiation ( $h\nu = 1486.6 \text{ eV}$ ). The X-ray gun was operated at 210 W (14 kV, 15 mA). The analyzer was operated in the FAT mode, with the pass energy set to 20 eV. For data acquisition and evaluation both manufacturer's (SpecsLab2) and commercial (CasaXPS, Origin) software were used. The binding energy scale was corrected by fixing the Ce 3d  $u'''$  peak to 916.6 eV or the Al 2p to 74.7 eV.

For XPS studies, the powder samples were pressed into pellets with ca. 1 cm diameter and a few tenth of mm thickness. Sample treatments were carried out in a high-pressure cell connected to the analysis chamber via a gate valve. After the pre-treatment, the samples were cooled down to room temperature in flowing nitrogen. Then, the high-pressure cell was evacuated; the sample was transferred to the analysis chamber in high vacuum (i.e., without contact to air), where the XP spectra were recorded.

Raman spectra of slightly pressed powder samples were measured in  $180^\circ$  backscattered geometry at 532 nm laser excitation (an incident laser power of 10 mW) using a Thermo Scientific DXR Raman microscope. Scans were integrated at  $4 \text{ cm}^{-1}$  resolution until the desired signal-to-noise ratio of 1000 or better was achieved (typically 30 s).

UV–vis diffuse reflectance spectroscopy (DRS) was employed to characterize the optical properties of the synthesized materials. The diffuse reflectance UV–vis spectra of the powdered samples were recorded by an

Avantes AvaSpec2048 Fiber Optic Spectrometer equipped with an Avasphere-50 type integrating sphere. The optical bandgap of the prepared materials was estimated by deriving the appropriate Tauc-plots using the following equation:

$$(h\nu\alpha)^{\frac{1}{n}} = A(h\nu - E_g)$$

where  $h$  is the Planck-constant,  $\nu$  is the photon frequency,  $\alpha$  is the absorption coefficient,  $A$  is a proportionality constant,  $E_g$  is the bandgap and  $n$  is a constant related to the nature of the electronic transition. All materials exhibited a direct transition, where  $n = 0.5$ .

X-ray diffractometry (Rigaku MiniFlexII; CuK $\alpha$ ) and electron diffraction technique were used for crystal structure and crystallinity determination. The ceria crystallites was determined by Scherrer's method for the (111) reflection.

Electrochemical measurements were performed on an Autolab PGSTAT302 instrument, in a classical one-compartment, three-electrode electrochemical cell. The various semiconductor nanoparticles were spray coated on Glassy carbon electrodes and were used as working electrodes. A large Pt foil counter-electrode and an Ag/AgCl/3 M KCl reference electrode completed the cell setup. The light source was a 300 W Hg–Xe arc lamp (Hamamatsu L8251). The radiation source was placed 2 cm away from the working electrode surface. Photovoltammetry profiles were recorded in 0.1 M Na<sub>2</sub>SO<sub>3</sub> electrolyte, using a slow potential sweep (2 mV s<sup>-1</sup>) in conjunction with interrupted irradiation (0.1 Hz) on the semiconductor coated electrodes. All the above procedures were performed at the laboratory ambient temperature (293 ± 2 K). For more experimental details see for example ref [27].

### 3 Results and Discussion

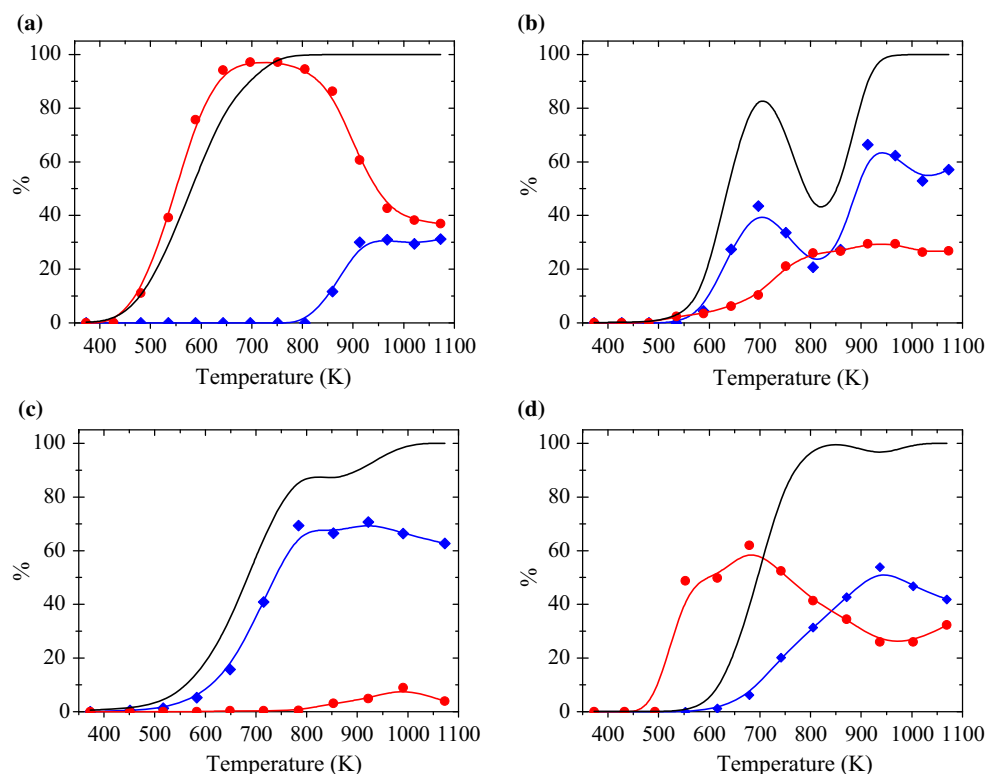
It turned out in former studies that small amounts of Rh additives (0.1–0.5 %) dramatically influenced the product formation in the CH<sub>4</sub>+CO<sub>2</sub> reaction on Co/alumina [15] and in the stream reforming of ethanol (SRE) on Co/ceria [19]; in both cases the selectivity of hydrogen significantly increased. In the SRE in the medium temperature range of 650–800 K practically only ethylene was detected on 2 % Co/alumina (Fig. 1a). Above 850 K, ethylene was still the dominant species, but H<sub>2</sub>, CO, CH<sub>4</sub>, acetaldehyde and a small amount of CO<sub>2</sub> were also formed. On 2 % Co/CeO<sub>2</sub>, at low conversion up to 500 K acetaldehyde and acetone were detected. From 500 to 700 K, the acetaldehyde selectivity attenuated the selectivities of H<sub>2</sub>, ethylene and CO<sub>2</sub> increased moderately and acetone was also present. At ~800 K, the conversion and the H<sub>2</sub> selectivity

transiently dropped, which was also seen as an increase in the acetaldehyde selectivity. A possible reason is the acetaldehyde desorption and recombination to ethanol [19]. Figure 1b shows the main products (hydrogen and ethylene). When 0.1 % Rh promoter was added the hydrogen selectivity markedly increased and ethylene formation significantly dropped (Fig. 1c). Between 600 and 800 K, small amounts of methane, CO, CO<sub>2</sub>, and acetaldehyde were also detected (not shown). It is important to mention that in presence of Rh acetone formation was not found. It is worthy of note that the by increasing the amount of cobalt to 10 %, the activity and hydrogen selectivity did not increase significantly [19]. For the CeO<sub>2</sub> support (without cobalt), initially only acetaldehyde was formed, but between 650–850 K the main product was ethylene (Fig. 1d) in contrast to the metal containing samples. From 700 to 900 K also other products such as acetone, hydrogen, CO<sub>2</sub>, CO, CH<sub>4</sub>, ethane and ethylene were formed. The presented catalytic data indicate that not only the acid–base character of support but the reducibility of the oxide and also the nature of interaction between the metals and the support are important.

In order to get closer to the understanding of the effect of Rh promoter in Co-based alumina and ceria catalysts we investigate the interaction of Rh and Co with the supports. The TPR, a dynamic method, gives information about the reducibility of the catalysts and helps identify the species formed after reduction in XPS. In Fig. 2a the TPR results of Al<sub>2</sub>O<sub>3</sub> supported Co–Rh catalysts are depicted. It can be seen that Rh in 1 % Rh/Al<sub>2</sub>O<sub>3</sub> becomes metallic at 395 K, but in the case of 2 % Co (curve b) hardly any peak corresponding to the reduction of Co oxides could be detected in the low temperature region. This is in agreement with the previous observation that at small metal contents probably mainly Co-aluminate compounds are formed with low reducibility, while at higher (10 w%) loading the Co<sub>3</sub>O<sub>4</sub> is dominant [28, 29]. Cobalt-support compounds can be formed during the catalytic reactions, too [30]. The only signal at 1187 K was attributed to the reduction of very small Co particles having strong interaction with Al<sub>2</sub>O<sub>3</sub> as well as to mixed metal-support oxides [31, 32]. After adding 0.1 % Rh to this sample, this process was enhanced and occurred at lower temperature. When the Rh content was increased to 1 %, two additional peaks were detected: the Rh was reduced at 421 K, and the Co at 569 K.

At 10 % Co content a broad feature with at least three components was detected, indicating the multiple mechanism of Co reduction over Al<sub>2</sub>O<sub>3</sub>. In general, TPR curves of Co/Al<sub>2</sub>O<sub>3</sub> samples in this region consists of two components: the reduction of Co<sub>3</sub>O<sub>4</sub> takes place first, followed by the CoO to Co<sup>0</sup> process [33]. This behavior is especially characteristic of the supported Co samples [34]. Taken into

**Fig. 1** H<sub>2</sub> (Diamond) and ethylene (Circle) selectivity data as well as EtOH conversion—during the SRE reaction over 2 % Co/Al<sub>2</sub>O<sub>3</sub> (a), 2 % Co/CeO<sub>2</sub> (b), 0.1 % Rh + 2 % Co/CeO<sub>2</sub> (c) and CeO<sub>2</sub> (d). Before catalytic test experiments the catalysts were reduced with H<sub>2</sub> at 773 K for 1 h. 1:3 ratio of ethanol–water was used



consideration the former results, we ascribe these features to the peaks located at 680 and 785 K, respectively. Components at lower temperatures can be the contributions of Co<sub>3</sub>O<sub>4</sub> particles having only weak interaction with the support [35]. When Rh was added, first an intensive peak emerged at 625 K next to the main peak at 785 K, then at 1 % Rh the maximum moved to 573 K, and only a shoulder remained at 647 K. The feature at 421 K originated from Rh.

From these results it can be concluded that by increasing the noble metal content, a systematic shift to lower temperatures was observed in case of the peak located above 1000 K. In the lower temperature region shifts and peak structure changes also took place. Fundamentally we attribute this enhanced reducibility to the H spill over phenomenon [23, 36]. However, on the basis of the XPS spectra, we suggest that Rh somehow weakens the interaction of Co with the support. Previously Ru and Pt have also been found to inhibit the formation of hardly reducible Co–Al<sub>2</sub>O<sub>3</sub> compounds [37, 38], and Rh was shown to hinder the dissolution of Co into the CeO<sub>2</sub> support [39]. That is why the reduction of the CoO–Al<sub>2</sub>O<sub>3</sub> compounds occurs sooner, and there are more available support-independent Co<sub>3</sub>O<sub>4</sub>. The forms of the oxides also differ at low and high metal contents.

On CeO<sub>2</sub> the Rh interacts with H<sub>2</sub> approximately at the same temperature as on Al<sub>2</sub>O<sub>3</sub>. The feature at 1080 K is

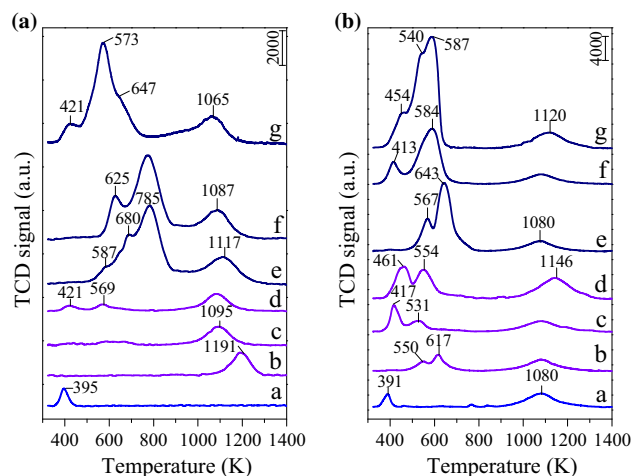


**Fig. 2** TPR results of Al<sub>2</sub>O<sub>3</sub> (a) and CeO<sub>2</sub> supported (b) Co–Rh catalysts: 1 % Rh (a), 2 % Co (b), 0.1 % Rh+2 % Co (c), 1 % Rh+2 % Co (d), 10 % Co (e) 0.1 % Rh+10 % Co (f) and 1 % Rh+10 % Co (g)

attributed to the bulk reduction of CeO<sub>2</sub> but the surface reduction at around 750–780 K is not well resolved on these samples [19], probably because the reducing effect of the metals could take place even during the preparation, before the reduction. Upon adding 2 or 10 % of Co, a well-resolved doublet was detected corresponding to the step-wise mechanism of Co<sub>3</sub>O<sub>4</sub> reduction, in the same

temperature range as on Al<sub>2</sub>O<sub>3</sub>. When the 2 % Co sample was promoted with 0.1 % Rh, the TPR peak of the Rh shifted to higher values. We suppose that it has some contribution from the Co, as only an additional minor peak could be seen at 531 K. In the case of 1 % Rh+2 % Co, the first peak moved to higher temperature and both peaks gained intensity.

By increasing the Co content, the reduction peaks moved to somewhat higher temperatures. In case of Co/Al<sub>2</sub>O<sub>3</sub> lower metal loading results in stronger interaction with the support, but with CeO<sub>2</sub> there is a different effect. In our former paper it was demonstrated that Co is well dispersed and upon reduction it dissolves into the support and disrupts it [39]. We also found that this phenomenon is enhanced at higher Co content. It means that CeO<sub>2</sub> will have larger surface (higher dispersity) to interact with Co at higher metal loadings.

When Rh was added to 10 % Co, its reduction took place at higher temperature (413 and 454 K) and the Co peak shifted to lower values (584 K at 0.1 % Rh, the two components are not resolved). On the 1 % Rh+10 % Co sample there is a significant intensity increase due to the enhanced reduction of Co<sub>3</sub>O<sub>4</sub>.

In general, the catalytic reaction take place at elevated temperatures. It has been shown that heating even in inert atmosphere induces oxidation state changes due to the enhanced oxygen mobility [39]. Thus, characterization should be done after higher temperature treatments to understand better the real catalysts.

The cobalt oxidation states were determined by XPS after reduction at 773 K. The Rh XPS was also monitored. The Rh enhanced reducibility was well detected. On 10 % Co supported over Al<sub>2</sub>O<sub>3</sub> (Fig. 3a) the Co 2p<sub>3/2</sub> component appeared at 781.3 eV with a satellite at 786.7 eV. The separation of the two 2p components was 15.7 eV. These features indicate the presence of Co<sup>2+</sup> compounds. When reduced, a new peak at 778.6 eV emerged due to the metallic Co. After the addition of 0.1 % Rh, the peak of the oxidized sample was located 0.8 eV lower than on the unpromoted one. In addition, the shake-up satellite significantly lost intensity and also shifted to lower values. The 1/2-3/2 peak separation was 15.2 eV, which is more characteristic of diamagnetic Co<sup>3+</sup> complexes [40, 41]. All these observations prove that after oxidation 10 % of Co is in Co<sup>2+</sup> state on Al<sub>2</sub>O<sub>3</sub>, but in the presence of Rh it forms preferably Co<sub>3</sub>O<sub>4</sub>. The formation of Co<sub>2</sub>RhO<sub>4</sub> in the reaction of Co<sub>3</sub>O<sub>4</sub> and Rh<sub>2</sub>O<sub>3</sub> cannot be excluded either [42]. However, its reduction after that is also promoted, as the metallic peak was more intensive. When reduced, the peak assigned to the oxidized state was also found Co<sup>3+</sup> like, which would indicate different surface reduction mechanisms with and without Rh. As the peak intensities did not change after Rh addition we exclude the possibility of

core-shell like structure. Rhodium at 0.1 % amount can be well dispersed over the whole surface, even in the Co-support interface, weakening their interaction.

When 10 % Co was supported on CeO<sub>2</sub>, after oxidation Co<sub>3</sub>O<sub>4</sub> was detected at 779.7 eV regardless of the Rh addition. When reduced, the promotion of Rh was evident from the higher intensity of the metallic peak (Co<sup>0</sup>) at 777.8 eV (Fig. 3b). The two-step reduction of Co<sub>3</sub>O<sub>4</sub> is indicated by the existence of the satellite on 10 % Co, and the higher CoO<sub>x</sub> binding energy on 0.1 % Rh + 10 % Co, that are characteristic of Co<sup>2+</sup>.

For the summarizing of the XPS data the surface metallic content with respect to the whole metallic content plus support molar content (M/(support +M)) were calculated. We also determined the ratio of metallic cobalt to all cobalt content (Co<sup>0</sup>/Co<sub>all</sub>). The data are collected in the Table 1. On alumina support the of Co<sup>0</sup>/Co<sub>all</sub> ratio increased from 11.3 to 25 % when the Co content was changed from 2 to 10 %. When 0.1 % Rh was added to 10 % Co this value increased slightly further to 28.6 %. Significantly higher promotional effect was observed on ceria support. In the case of 0.1 % Rh+10 % Co/CeO<sub>2</sub>, the Co<sup>0</sup>/Co<sub>all</sub> is 53.1 % comparing to the 10 % Co/CeO<sub>2</sub> where this value is only 33.1 %. The other important observation is that the Rh enriches on the surface. While the Rh/(support +M<sub>all</sub>) is 0.5 % on 0.1 % Rh/CeO<sub>2</sub>, this value is significantly higher, 3.8 % on 0.1 % Rh+10 % Co/CeO<sub>2</sub>. Such kind of enrichment was not calculated for Co (see Table 1). We may conclude that the increased number of Rh atoms and the presence of metallic Co species are responsible for the higher catalytic activity. It is important to emphasize that the formation of metallic sites are

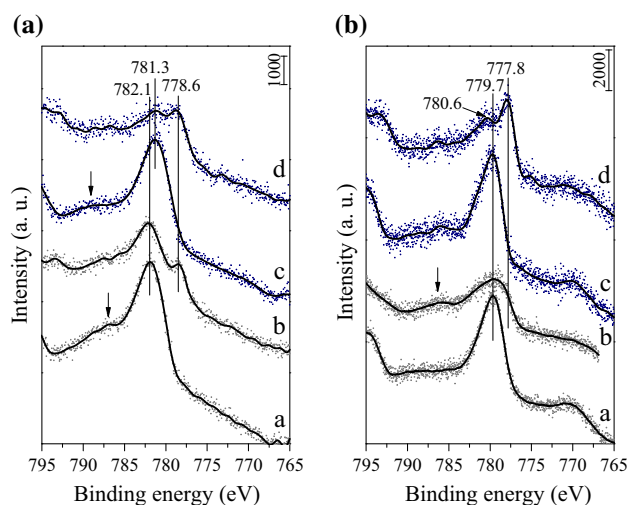


**Fig. 3** XP spectra of Al<sub>2</sub>O<sub>3</sub> (a) and CeO<sub>2</sub> (b) supported catalysts after oxidation at 673 K for 30 min and after reduction at 773 K for 1 h. 10 % Co oxidized (a) and reduced (b), 0.1 % Rh+10 % Co oxidized (c) and reduced (d)

necessary for C–C bond rupture in SRE on ceria supported catalysts which finally leads to hydrogen production [19, 23, 42].

The catalytic results show that the character of the support has a great influence on the SRE catalysis; using acidic support like alumina, the ethylene formation is favorable, while on basic ceria supported catalysts, other routes, including hydrogen formation are allowed [6, 19]. On the other hand the metals (in the present case Rh and Co) have influence on the reducibility of the support (in the present case on ceria). XPS results (Table 2) show that the Rh and Co (and Rh+Co) interact with ceria and increase its reducibility. XRD experiments pointed out that Co induces the disruption of ceria, its particle size decreased dramatically (Table 2). We suppose that the change of particle size of ceria also has an effect for catalytic activity of Co-based ceria catalysts.

We believe that beside the increased number of atoms in metallic state in the surface layer, the defect concentration and changes in Fermi level region may also contribute to the observed catalytic effects. In order to get more information about this phenomenon, some Raman measurements were carried out on 1 % Rh and 2 % Co samples reduced at different temperatures. In Fig. 4 the reference spectrum of CeO<sub>2</sub> can be seen, with a narrow peak at 464 cm<sup>-1</sup> corresponding to the triply degenerate F<sub>2</sub> g mode of CeO<sub>2</sub> with fluorite structure. After the addition of either Co or Rh this feature significantly broadened and shifted to 439 cm<sup>-1</sup>. In addition, new peaks and shoulders appeared at 225 (2TA mode), 602 (defect induced, D mode) and 1175 cm<sup>-1</sup> (2LO mode) that we attribute definitely to the effect of metals. It could indicate metal ion incorporation, O vacancy formation and particle size decrease [43]. Our spectra show very similar structure in every case, suggesting that the reduction temperature and the type of the metal defect have minor effect on the final

defect concentration, although Rh and Co interacts differently with CeO<sub>2</sub>.

The value of the bandgap is also a very important property of the catalytic systems. It has been presented that the addition of doping agents or the formation of Ce<sup>3+</sup> centers decreases the bandgap [44]. A decreased bandgap in partially reduced CeO<sub>2</sub> and its enhanced photocatalytic activity has already been published, too [45, 46]. In our samples untreated CeO<sub>2</sub> had intensive absorption at 3.71 eV (Fig. 5). When 1 % Rh, 2 % Co or 1 % Rh+2 % Co were added, additional absorptions appeared at lower energies attributed to both the plasmonic effect of the metal nanoparticles, and the eventually formed midgap states of CeO<sub>2</sub>. Because the local maxima were located at the same positions in all samples, we suppose that this feature is primarily caused by the defect structure of CeO<sub>2</sub>. In line with that XPS confirmed higher Ce<sup>3+</sup> ratio in the presence of the metals; for pure CeO<sub>2</sub> it was 10 %, and in the 1 % Rh+2 % Co/CeO<sub>2</sub> it was 15 % (Fig. 5b), thus the addition of the metals alters significantly the CeO<sub>2</sub> surface structure and its catalytic properties (Fig. 1). We suppose that for the observation of Rh plasmonic feature our metal particles are too small [47, 48]. The incorporation of metal ions would suppress the Ce<sup>3+</sup> formation by replacing it and the corresponding absorptions decrease [49, 50]. In our case this can be ruled out as an opposite trend of the intensities was observed. As we postulated in our previous work [39], after the reduction of Co/CeO<sub>2</sub> the majority of Co remains in ionic state. Part of the absorption feature at around 550–600 nm may contain some Co<sup>2+</sup> contribution (Fig. 5a). Recently it was found that the attachment of Co<sup>2+</sup> onto TiO<sub>2</sub> nanorod produced an absorption maximum at ~580 nm in the UV–Vis absorbance spectrum [51].

The direct bandgaps of CeO<sub>2</sub>, 1 % Rh/CeO<sub>2</sub> and 2 % Co/CeO<sub>2</sub> varied around 3.27 eV. The high non-characteristic absorption made it impossible to calculate the bandgap of 1 % Rh + 2 % Co/CeO<sub>2</sub>.

**Table 1** Metallic contents and the Co<sup>0</sup>/Co<sub>all</sub> ratio on the different catalysts calculated from the XP spectra

Samples	M/(support+M)	Co <sup>0</sup> /Co <sub>all</sub>
2 % Co/CeO <sub>2</sub>	3.3	25.8
10 % Co/CeO <sub>2</sub>	14.0	33.1
0.1 % Rh/CeO <sub>2</sub>	0.5	–
1 % Rh/CeO <sub>2</sub>	2.2	–
0.1 % Rh+2 % Co/CeO <sub>2</sub>	5.4 (Co) 2.0 (Rh)	29.1
0.1 % Rh+10 % Co/CeO <sub>2</sub>	13.4 (Co) 3.8 (Rh)	53.1
2 % Co/Al <sub>2</sub> O <sub>3</sub>	1.9	11.3
10 % Co/Al <sub>2</sub> O <sub>3</sub>	2.5	25.0
0.1 % Rh+10 % Co/Al <sub>2</sub> O <sub>3</sub>	1.7 (Co)	28.6

**Table 2** Ceria reducibility (Ce<sup>3+</sup>/Ce<sub>all</sub>) and CeO<sub>2</sub> particle size on different catalysts

Samples	Ce <sup>3+</sup> /Ce <sub>all</sub>	CeO <sub>2</sub> particle size (nm)
CeO <sub>2</sub>	11	27.6
2 % Co/CeO <sub>2</sub>	10	17.1
10 % Co/CeO <sub>2</sub>	14	10.7
0.1 % Rh/CeO <sub>2</sub>	12	27.6
1 % Rh/CeO <sub>2</sub>	15	26.7
5 % Rh/CeO <sub>2</sub>	16	26.5
0.1 % Rh+2 % Co/CeO <sub>2</sub>	14	17.0
0.1 % Rh+10 % Co/CeO <sub>2</sub>	17	11.1
1 % Rh+2 % Co/CeO <sub>2</sub>	15	24.1

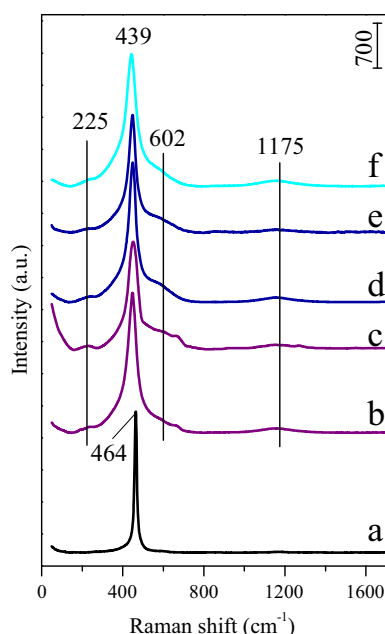


**Fig. 4** Raman spectra of CeO<sub>2</sub> (a), 2 % Co/CeO<sub>2</sub> reduced at 423 K (b) and 773 K (c), 1 % Rh reduced at 423 K (d) and 773 K (e), 1 % Rh+2 % Co reduced at 423 K (f)

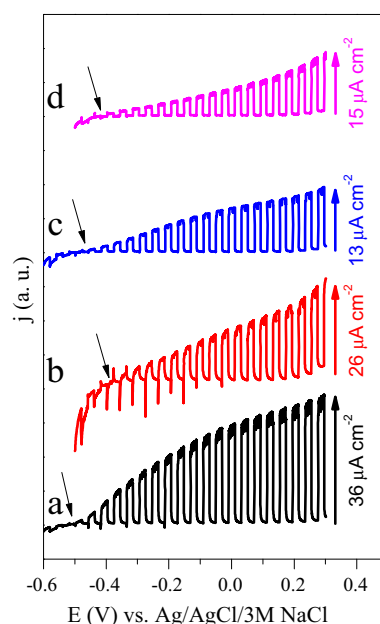


**Fig. 6** Photovoltammometry profiles of CeO<sub>2</sub> (a), 1 % Rh/CeO<sub>2</sub> reduced at 423 K (b), 2 % Co/CeO<sub>2</sub> reduced at 773 K (c), and 1 % Rh+2 % Co/CeO<sub>2</sub> reduced at 773 K (d) recorded in 0.1 M Na<sub>2</sub>SO<sub>3</sub> solution at a sweep rate of 2 mV.s<sup>-1</sup>

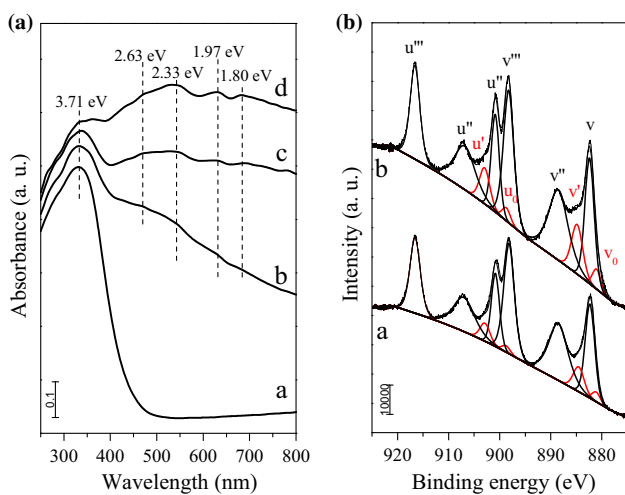


**Fig. 5** UV-vis absorption spectra (a) of CeO<sub>2</sub> (a), 1 % Rh/CeO<sub>2</sub> reduced at 423 K (b) 2 % Co/CeO<sub>2</sub> reduced at 773 K (c) and 1 % Rh+2 % Co/CeO<sub>2</sub> reduced at 773 K (d). Ce 3d spectra (b) of CeO<sub>2</sub> and 1 % Rh+2 % Co/CeO<sub>2</sub> after reduction at 773 K

In our previous work [39, 52] we demonstrated that after the reduction of ceria supported Rh and Co samples, enhanced surface reduction of the support was observed. In accordance with this fact Fig. 5b shows that Co and Rh together could increase considerably the number of Ce<sup>3+</sup> species on the surface. In this process the surface diffusion may play an important role [38]. Taking into account the Raman and optical results, we propose that the density of

the surface defects over CeO<sub>2</sub> depends on the metal quantity, rather than on the type of the metal.

Figure 6 clearly shows that all samples behave as n-type semiconductors with the photocurrent signals anodic in polarity. The photocurrent density of CeO<sub>2</sub> slightly decreased when the metal nanoparticles were added. It means that the separation of the photoexcited electron-hole pairs worsened, especially in the presence of Co [53]. More importantly, the onset potential of the photovoltammogram can be used to estimate the Fermi level of the n-CeO<sub>2</sub> [27]. Thus the position of the conduction band edge was estimated for all the samples. The fact that there is a considerable shift in the Fermi level in the case of the metal containing samples (50, 150, 80 mV for Co, Rh, and Co/Rh, respectively) indicate an intimate contact between the CeO<sub>2</sub> and the metal particles allowing a certain extent of Fermi-level equilibration [54].

## 4 Summary

Al<sub>2</sub>O<sub>3</sub> and CeO<sub>2</sub> supported Co catalyst were characterized with and without Rh promoter. TPR and XPS results revealed that Rh fundamentally changed the reduction mechanism of Co: not only the reduction took place at lower temperatures, but the intermediate Co forms were different. Moreover, Rh inhibits the formation of strong Co-support interaction. Using ceria support we may

conclude that the Rh enrichment in the surface layer and the presence of metallic Co are responsible for the higher catalytic conversion and for the enhanced hydrogen selectivity in the SRE reaction. Over the n-type semiconductor CeO<sub>2</sub> metal induced defects were evidenced by Raman spectroscopy and DRS. Co and Rh did not change the bandgap, but metal-support electronic interaction was observed by photovoltammetry. Comparing the catalytic results with the catalyst characterization results, we suppose that in addition to the presence of the metals, the metal induced changes on the support surface, like increased O-vacancy density and Fermi-level equilibration also influence the catalytic process.

**Acknowledgments** The authors acknowledge Dr. Csaba Janáky for the discussion about the photoelectrochemical results and Levente Koppány Juhász for the Raman spectroscopic measurements.

## References

- Breyse M, Afanasiev P, Geantet C, Vrinat M (2003) *Catal Today* 86:5–16
- Saeidi S, Amin NAS, Rahimpour MR (2014) *J CO<sub>2</sub> Util* 5: 66–81
- Enger BC, Lodeng R, Holmen A (2010) *Catal Lett* 134:13–23
- Pusztai P, Puskás R, Varga E et al (2014) *Phys Chem Chem Phys* 16:26786–26797
- Mullins DR (2015) *Surf Sci Rep* 70:42–85
- Mattos LV, Jacobs G, Davis BH, Noronha FB (2012) *Chem Rev* 112:4094–4123
- Liu W, Flytzani-Stephanopoulos M (1995) *J Catal* 153:317–332
- Rodríguez JA, Liu P, Hrbek J, Evans J, Manuel P (2007) *Angew Chem Int Ed* 46:1329–1332
- Mullins DR, Albrecht PM, Chen T-L et al (2012) *J Phys Chem C* 116:19419–19428
- Guczi L, Boskovic G, Kiss E (2010) *Chem Rev* 52:133–203
- Zhang Y, Chen L, Bai G, Li Y, Yan X (2005) *J Catal* 236:176–180
- Riedel T, Claeys M, Schulz H et al (1999) *Appl Catal A* 186:201–213
- Melaet G, Lindeman AE, Somorjai GA (2014) *Top Catal* 57:500–507
- Chu W, Chernavskii PA, Gengembre L, Parkina GA, Fongarland P, Khodakov AY (2007) *J Catal* 252:215–230
- Ferencz Z, Baán K, Oszkó A, Kónya Z, Kecskés T, Erdőhelyi A (2014) *Catal Today* 228:123–130
- Ruckenstein E, Wang HY (2002) *J Catal* 205:289–293
- Badlani M, Wachs IE (2001) *Catal Lett* 75:137–149
- Tóth M, Varga E, Oszkó A, Baán K, Kiss J, Erdőhelyi A (2016) *Appl Catal A* 411:377–387
- Ferencz Z, Erdőhelyi A, Baán K, Oszkó A, Óvári L, Kónya Z, Papp C, Steinrück H-P, Kiss J (2014) *ACS Catal* 4:1205–1218
- Martono E, Vohs JM (2012) *J Catal* 291:79–86
- Batista MS, Santos RKS, Assaf EM, Assaf JM, Ticianelli EA (2003) *J Power Sources* 124:99–103
- Lin SSY, Kim DH, Engelhard MH, Ha SY (2010) *J Catal* 273:229–235
- Varga E, Ferencz Z, Oszkó A, Erdőhelyi A, Kiss J (2015) *J Mol Catal A* 397:127–133
- Profeti LPR, Ticianelli EA, Assaf EM (2008) *J Power Sources* 175:485–489
- Espinal R, Taboada E, Molins E, Chimentao RJ, Medina F, Llorca J (2013) *Top Catal* 56:1660–1671
- Pereira EB, Piscina PR, Marti S, Homs N (2010) *Energy Environ Sci* 3:486–492
- Kormányos A, Thomas A, Huda MN, Sarker P, Liu JP, Poudyal N, Janáky C, Rajechwar K (2016) *J Phys Chem C*. doi:10.1021/acs.jpcc.1025b12738
- Chin RL, Hercules DM (1982) *J Phys Chem* 86:360–367
- Liotta LF, Carlo GD, Pantaleo G, Venezia AM, Deganello G (2006) *Appl Catal B* 66:217–227
- Jacobs G, Ma W, Davis BH (2014) *Catalysts* 4:49–76
- Ali S, Zabidi NAM, Subbarao D (2011) *Chem Cent J* 5:68
- Das TK, Jacobs G, Patterson PM, Conner WA, Li J, Davis BH (2003) *Fuel* 82:805–815
- Ewbank JL, Kovarik L, Kenvina C, Sievers C (2014) *Green Chem* 16:885–896
- Bulavchenko OA, Cherepanova SV, Malakhov VV, Dovlitova LS, Ishchenko AV, Tsybulya SV (2009) *Kinet Catal* 50:192–198
- Simionato M, Assaf EM (2003) *Mater Res* 6:535–539
- Cook KM, Poudyal S, Miller JT, Bartholomew C, Hecker WC (2012) *Appl Catal A* 449:69–80
- Kogelbauer A, Goodwin JGG, Oukaci R (1996) *J Catal* 160:125–133
- Guczi L, Hoffer T, Zsoldos Z, Zyade S, Maire G, Garin F (1991) *J Phys Chem* 95:802–808
- Varga E, Pusztai P, Óvári L, Oszkó A, Erdőhelyi A, Papp C, Steinrück H-P, Kónya Z, Kiss J (2015) *Phys Chem Chem Phys* 17:25166–27157
- Frost CD, McDowell CA, Woolsey IS (1972) *Chem Phys Lett* 17:320–323
- Schmid M, Kaftan A, Steinrück HP, Gottfried JM (2012) *Surf Sci* 606:945–949
- Cascales C, Rasines I (1984) *Mater Chem Phys* 10:199–203
- Daniel M, Lorient S (2012) *J Raman Spectrosc* 43:1312–1319
- Khan MM, Ansari SA, Pradhan D, Han DH, Lee J, Cho MH (2014) *Ind Eng Chem Res* 53:9754–9763
- Aslam M, Oamar MT, Soomro MT, Ismail IMI, Salah N, Almeelbi T, Gonda A, Hameed A (2016) *Appl Catal B* 180:391–402
- Verma R, Samdarshi SK, Bojja S, Paul S, Choudhury B (2015) *Sol Energ Mater Sol Cells* 141:414–422
- Watson AM, Zhang X, de la Osa RA, Sanz JM, González F, Moreno F, Finkelstein G, Liu J, Everitt HO (2015) *Nano Lett* 15:1095–1100
- Zhang X, Li P, Barreda A, Gutiérrez Y, González F, Moreno F, Everitt HOJ (2016) *Nanoscale Horiz* 1:75–80
- Balestrieri M, Colis S, Gallart M, Schember G, Ziegler M, Gilliot P, Dinia A (2015) *J Mater Chem C* 3:7014–7021
- Wang Z, Quan Z, Lin J (2007) *Inorg Chem* 46:5237–5242
- Balasanthiran C, Hoefelmeyer JD (2014) *Chem Commun* 50:5721–5724
- Varga E, Pusztai P, Oszkó A, Baán K, Erdőhelyi A, Kónya Z, Kiss J (2016) *Langmuir* 32:2761–2770
- Li B, Gu T, Wang J, Wang P, Wang J, Yu JC (2014) *ACS Nano* 8:8152–8162
- Subramanian V, Wolf EE, Kamat VP (2004) *J Am Chem Soc* 126:4943–4950